

Seasonal subsidence and rebound in Las Vegas Valley, Nevada, observed by synthetic aperture radar interferometry

Jörn Hoffmann and Howard A. Zebker

Department of Geophysics, Stanford University, Stanford, California

Devin L. Galloway

U.S. Geological Survey, Sacramento, California

Falk Amelung

Hawaii Institute of Geophysics and Planetology, University of Hawaii, Honolulu, Hawaii

Abstract. Analyses of areal variations in the subsidence and rebound occurring over stressed aquifer systems, in conjunction with measurements of the hydraulic head fluctuations causing these displacements, can yield valuable information about the compressibility and storage properties of the aquifer system. Historically, stress-strain relationships have been derived from paired extensometer/piezometer installations, which provide only point source data. Because of the general unavailability of spatially detailed deformation data, areal stress-strain relations and their variability are not commonly considered in constraining conceptual and numerical models of aquifer systems.

Interferometric synthetic aperture radar (InSAR) techniques can map ground displacements at a spatial scale of tens of meters over 100 km wide swaths. InSAR has been used previously to characterize larger magnitude, generally permanent aquifer system compaction and land subsidence at yearly and longer timescales, caused by sustained drawdown of groundwater levels that produces intergranular stresses consistently greater than the maximum historical stress. We present InSAR measurements of the typically small-magnitude, generally recoverable deformations of the Las Vegas Valley aquifer system occurring at seasonal timescales. From these we derive estimates of the elastic storage coefficient for the aquifer system at several locations in Las Vegas Valley. These high-resolution measurements offer great potential for future investigations into the mechanics of aquifer systems and the spatial heterogeneity of aquifer system structure and material properties as well as for monitoring ongoing aquifer system compaction and land subsidence.

1. Introduction

During the past several decades, Las Vegas, Nevada, (Figure 1) has experienced significant land subsidence due to compaction of the aquifer system. Though groundwater level declines had become apparent by 1912 [Maxey and Jameson, 1948] owing to discharging wells since the late 1800s, accelerated groundwater pumping since the late 1940s to provide water for the currently fastest growing metropolitan area in the United States (U.S. Department of Commerce, Metropolitan area rankings by population size and percent change: 1990 to 1999, available at <http://www.census.gov/population/www.estimates/metropop.html>, 1999) has lowered aquifer hydraulic heads over the entire valley. Maximum groundwater level declines in some areas exceeded 70 m between 1912 and 1972 [Morgan and Dettinger, 1991], and by 1990 the maximum decline exceeded 90 m [Burbey, 1995], although water levels had begun to recover in some areas. In 1998, accounting for artificial recharge of imported surface water, groundwater constituted ~14% of the municipal water supply [Coache, 1999]. The re-

mainder was met with water imported from Lake Mead. In the central part of the valley, declining heads in the aquifer system incorporating thick, highly compressible clay beds (aquitards) have led to subsidence rates of several centimeters per year during most of the 20th century, with resulting damage to structures and well casings. Differential subsidence has reactivated existing Quaternary faults and created new earth fissures [Bell and Price, 1991]. Recently, artificial recharge has become an increasingly important tool to mitigate the negative effects of land subsidence due to overdrafting of the aquifer system in Las Vegas [Pavelko *et al.*, 1999].

Subsidence in the Las Vegas area has previously been monitored using precise leveling surveys and a borehole extensometer installation, the Lorenzi site, that was installed in 1994 [Pavelko, 2000]. Recently, Amelung *et al.* [1999] studied multi-year subsidence in Las Vegas Valley between 1992 and 1997 using interferometric synthetic aperture radar (InSAR) techniques and satellite-borne synthetic aperture radar data. They delineated a subsidence bowl in northwest Las Vegas Valley, where a maximum subsidence of 190 mm was measured between April 1992 and December 1997, and a central subsidence zone around the downtown area, where the maximum measured subsidence was ~110 mm in that time period. These results extended and enhanced the definition of these features,

Copyright 2001 by the American Geophysical Union.

Paper number 2000WR900404.
0043-1397/01/2000WR900404\$09.00

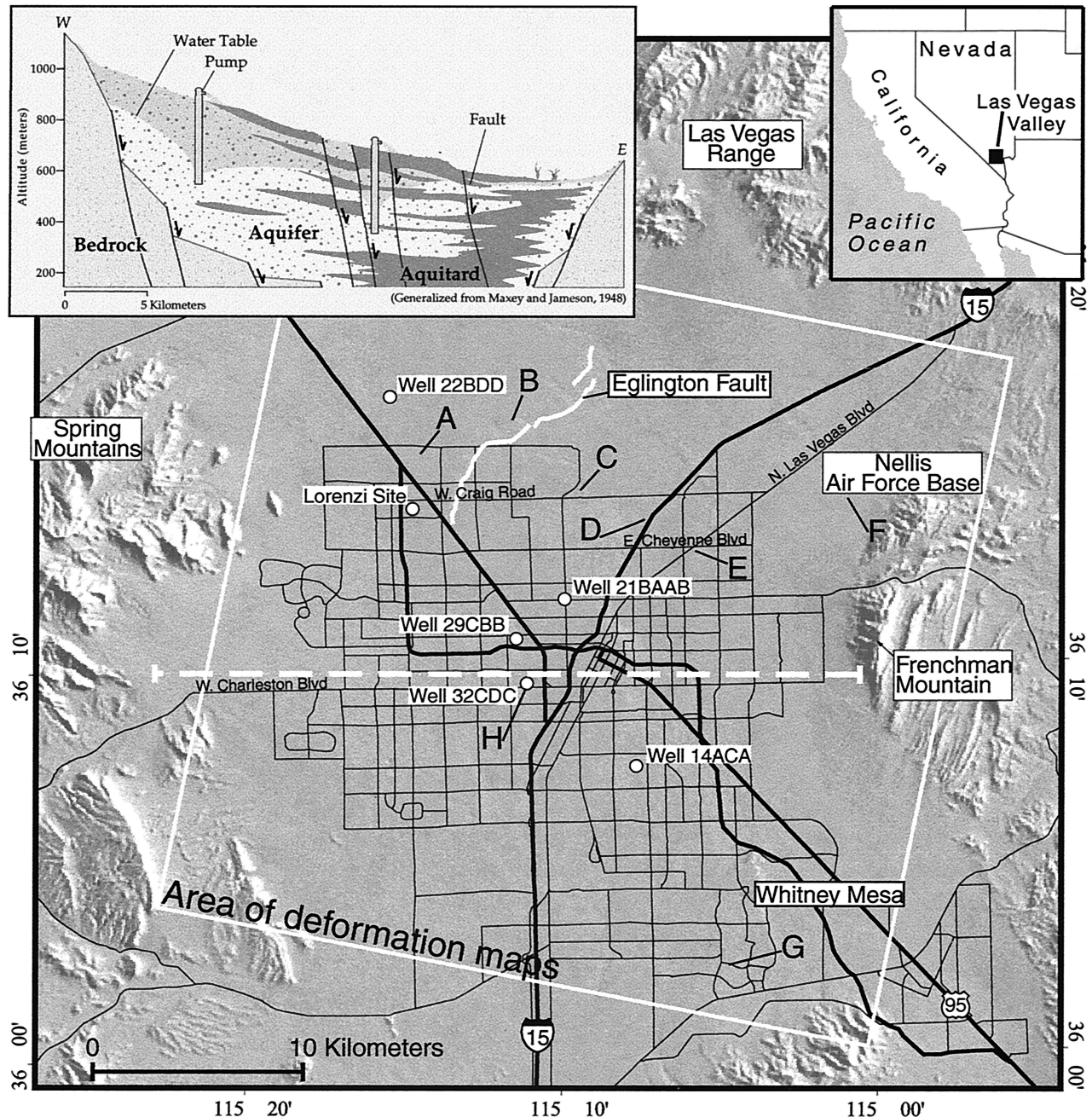


Figure 1. Location map of Las Vegas Valley. The white frame indicates the area displayed in Plates 1, 2, and 3. The letters A–H label the same areas as in the displacement maps. The well and extensometer locations are shown as white dots. The inset on the top left shows a generalized stratigraphic cross section along the profile shown on the map (white dashed line).

which had been previously mapped by leveling surveys in 1963 and 1987 [Bell and Price, 1991]. In addition, the InSAR imagery revealed that the Quaternary Eglinton fault controls the spatial extent of the observed subsidence pattern along the southeastern boundary of the northwest subsidence bowl. The 1992–1997 subsidence rates in the northwest subsidence bowl are significantly smaller than the 50 mm yr^{-1} measured from 1980 to 1982 by Bell and Price [1991]. Amelung *et al.* [1999] explained differences between interferograms spanning more than 1 year with differences in the contributions of periods of seasonal water level recovery relative to periods of water level

decline. Interferograms that contained more winter season recovery showed less subsidence or relative uplift, while those with relatively more summer season decline showed more subsidence. However, they did not investigate the seasonal changes in the observed displacement patterns in detail or compare their magnitude to the observed multiyear subsidence.

Galloway *et al.* [1998] speculated that seasonal InSAR-derived displacement maps could be used in conjunction with hydraulic head measurements to compute the elastic storage coefficient of confined aquifer systems undergoing significant

seasonal deformation (>10 mm). Under the favorable radio-metric conditions in Las Vegas Valley, relatively small (≥ 5 mm) poroelastic deformations of the aquifer system in response to changes in aquifer head can be detected by InSAR within 1 month of the onset of the rapid drawdown and recovery of groundwater levels in response to the annual cycle of summer pumping and winter recharge. This capability, in addition to the importance of the valley fill aquifer system to the Las Vegas community, make this an interesting area of study.

The lack of spatially detailed hydrogeologic and geodetic information has limited the study of spatial heterogeneity in aquifer systems, which has been recognized to be an important factor in mitigating negative consequences of overdrafting [e.g., *Carrillo-Rivera*, 1999]. In this work, we will present displacement maps derived from spaceborne radar measurements acquired by the European Remote Sensing satellites ERS-1 and ERS-2. These measurements can yield surface displacements accurate to subcentimeter levels at a spatial resolution of 20 m, over swaths 100 km in extent. The extensive coverage of Las Vegas Valley by the ERS satellites constitutes a catalog of accurate displacement measurements at unprecedented spatial resolution. It is our intent here to use these data to address the mechanics of deforming aquifer systems, and the controlling hydrogeologic parameters, in their spatial detail. This new constraint for hydrogeologic models promises to yield more information on the storage properties of the aquifer system. A better understanding of the areal variability of the aquifer system response to stress will be very useful in refining existing groundwater flow models and can improve the effectiveness of groundwater management schemes. It may further enable the identification of zones with a high potential of fissure formation, which would be valuable information in city planning.

The purpose of this paper is threefold. First, we explicitly address seasonal-scale deformation in Las Vegas Valley by creating interferograms with temporal baselines on the order of a few months. Second, we document land subsidence during 1997–1999. Third, we use the InSAR-derived displacements and water level variations to obtain an estimate of the elastic storage coefficients at six locations in the Las Vegas Valley aquifer system.

2. Aquifer System Deformation

An unconsolidated alluvial aquifer system typically constitutes a series of relatively flat lying aquifers interbedded with aquitards that confine fluid pressures in the underlying aquifers. Land subsidence caused by the compaction of overdrafted aquifer systems occurs as a result of consolidation of the aquitards (compressible silt and clay deposits) within the aquifer system. The theory of poroelasticity, as first conceptualized by *Terzaghi* [1925] in one dimension and later extended to three dimensions by *Biot* [1941], requires that fluctuations in pore pressure cause stress changes in the porous material. According to *Terzaghi's* [1925] principle of effective stress the total stress, σ_T , on the confined aquifer system is equal to the sum of the pore pressure, p , and the effective or intergranular stress, σ_e , or in terms of the effective stress,

$$\sigma_e = \sigma_T - p. \quad (1)$$

The total stress is the weight of the overlying fluid and geologic medium. Under this principle, for the simplified case where the total stress remains constant, a change in pore pressure is

accompanied by an equal magnitude but oppositely sensed change in effective stress. Decreasing pore pressures cause increasing effective stresses, which act to compress the granular skeleton of the aquifer or aquitard. Conversely, increasing pore pressures are accompanied by expansion of the granular skeleton.

If the change in effective stress, $\Delta\sigma_e$, is due solely to a change in fluid pressure, Δp , and not to a change in lithostatic stress, $\Delta\sigma_e$ can be determined from measurements of fluid pressure or hydraulic head fluctuations, $\Delta h = \Delta p/(\rho g)$, in wells tapping the aquifer system. For this case, an elastic skeletal storage coefficient, S_{ke}^* , can be calculated for the aquifer system [Riley, 1969]:

$$S_{ke}^* = \frac{\Delta b^* \rho g}{\Delta p} = \frac{\Delta b^*}{\Delta h}, \quad (2)$$

where Δb^* is the change in thickness of the aquifer system, ρ is the density of water, and g is the gravitational acceleration. The elastic skeletal storage coefficient is the change in pore volume in the saturated portion of an aquifer system per unit area and unit change in hydraulic head, attributed to purely elastic deformation. For aquifer systems that constitute heterogeneous unconsolidated alluvial deposits, S_{ke}^* typically is 2.5 to 5 times larger than S_w^* (the storage coefficient related to the compressibility of water); therefore S_{ke}^* constitutes roughly 70 to 85 percent of S^* (the elastic storage coefficient of the aquifer system). We use S^* to denote the property of the aquifer system as a whole, as opposed to S , which is the storage coefficient of the aquifer as defined by *Jacob* [1950]. However, if head decline produces effective stresses greater than the maximum historical stress, the sediments undergo irreversible compaction, largely concentrated in the aquitards. For these stresses an inelastic storativity governs the compaction of the aquitards, and its value is typically 20 to more than 100 times larger than the elastic value [Riley, 1998]. A more detailed discussion of the various storage coefficients can be found in Appendix A.

The elastic storage coefficient of aquifer systems is a bulk value that reflects the responses of the aquifer and aquitard fractions of the aquifer system to variations in head in those units. It is a critical hydraulic parameter that strongly influences the nonsteady flow of groundwater and is important to groundwater resource evaluations. Typically, these bulk values of the storage coefficient may be difficult to obtain and of questionable reliability. In situ values can be obtained from measurements of drawdown rates in pumping tests, but these can be costly and often are representative of only the most permeable fraction of the aquifer system, the aquifers. Values can also be measured in the laboratory from core samples, but these measurements generally are not representative of in situ conditions [Riley, 1998]. Most often the aquifer storage coefficient is estimated from the “rule-of-thumb” relation, $S = 3 \times 10^{-6} b^*$, where b^* is the saturated aquifer thickness in meters [Todd, 1980].

We show in section 7 that seasonal InSAR-derived displacement maps of Las Vegas Valley (measuring Δb), in conjunction with groundwater levels (measuring Δh), can yield spatially varying estimates of storage coefficients for those parts of the aquifer system undergoing largely elastic deformation. It is typically assumed that deformation within the aquifer system is purely elastic when and where the previous maximum stress is not exceeded [Poland, 1961]. We focus on areas where the annual and multiyear interferograms show no net subsidence.

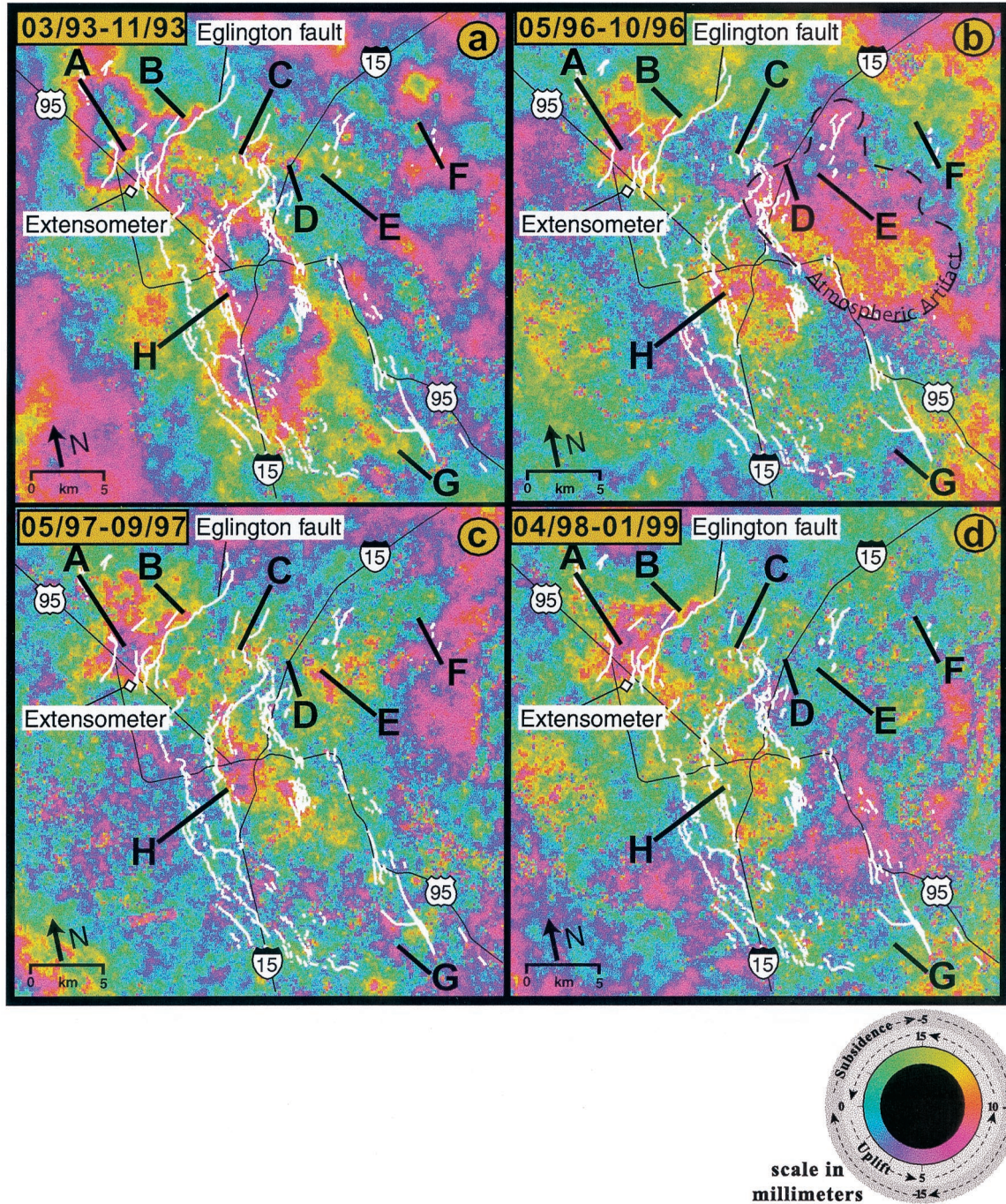


Plate 1. Comparison of the displacement patterns for four summer seasons: (a) March 1993 to November 1993, (b) May 1996 to October 1996, (c) May 1997 to September 1997, and (d) April 1998 to January 1999. Uplift and subsidence are determined by the order of the colors: Uplift is characterized by blue-red-yellow-green-blue and subsidence is displayed with the reverse color order (see color scale). Plate 1d also contains a significant part of a winter season. Most large-scale patterns recur in all images, even though they exhibit varying magnitudes. Subsidence rates are generally decreasing in recent years. The large uplift seen in the eastern part of outlined pink color in Plate 1b is an atmospheric artifact. The northwest subsidence bowl includes areas A and B.

This suggests that the stresses fluctuate in the elastic range, and inelastic residual compaction of thick aquitards is negligible. In overdrawn, subsiding groundwater basins, delays in dissipation of residual excess pore pressure in the thicker aquitards introduce a major time delay between changes in hydraulic head in the aquifers and the deformation in the aquitards.

These delays have been described by a time constant for the system, defined as the time after which 93% of the ultimate compaction has occurred in an aquitard under a step decrease of hydraulic head in two bounding aquifers [Riley, 1969]. For aquitards several meters to several tens of meters thick these time constants can be decades to centuries [Ireland *et al.*, 1984],

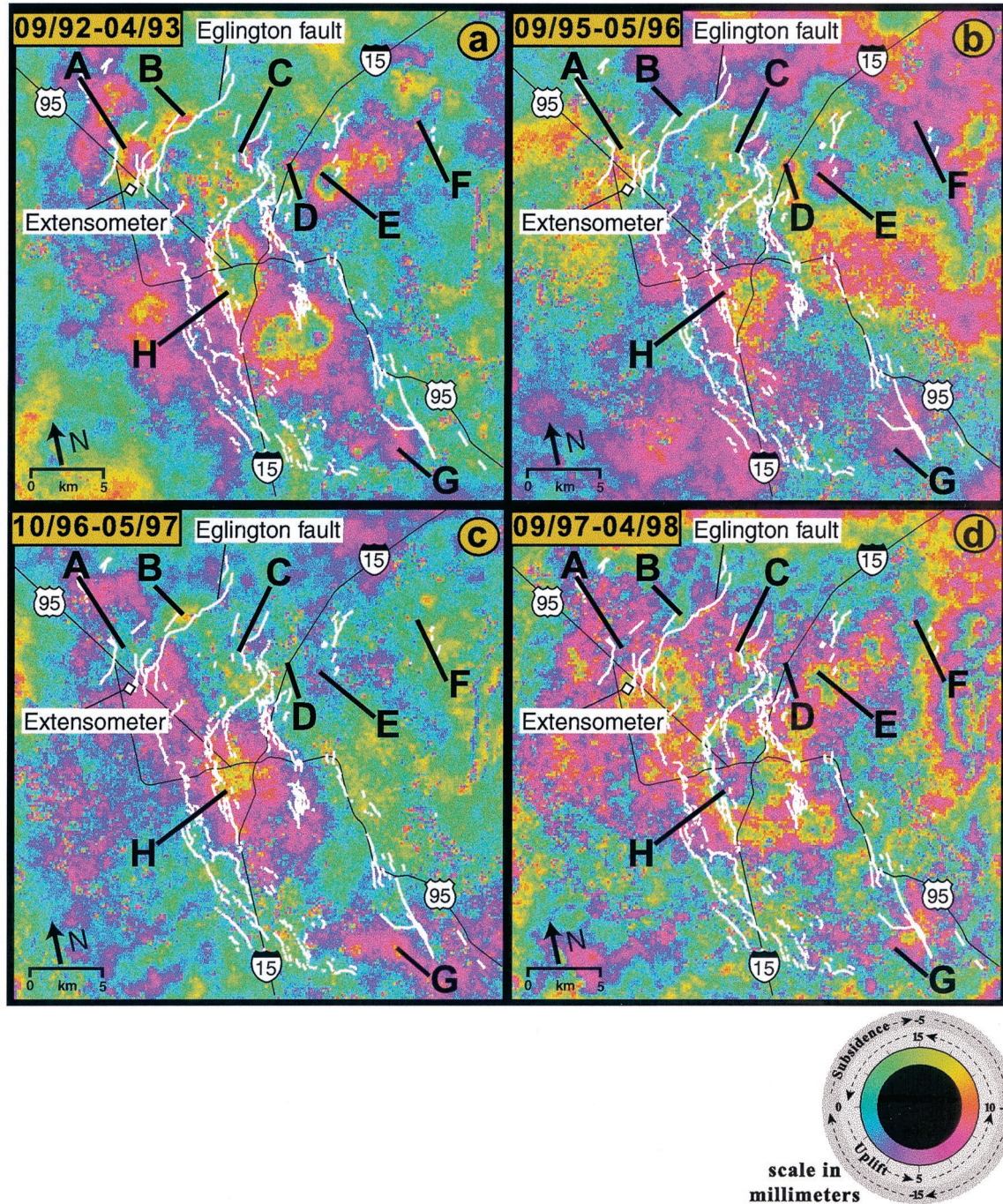


Plate 2. Displacement patterns for four winter seasons: (a) September 1992 to April 1993, (b) September 1995 to May 1996, (c) October 1996 to May 1997, and (d) September 1997 to April 1998. The dominant deformation observed is uplift in the central subsidence zone. The subsidence in the northwest subsidence bowl (areas A and B) has almost entirely vanished in recent years. Note that the uplift in Plate 2d is significantly stronger than in Plates 2b and 2c and also somewhat larger than in Plate 2a.

leading to continuing residual compaction occurring long after the heads in the aquifers have ceased declining or have, in fact, recovered significantly. Except for one location, the site of a borehole extensometer ("Lorenzi site," Figure 1), our analyses were focused on areas where we observed only small inelastic residual compaction trends. It should be noted, however, that even under elastic conditions in the aquifer system, time lags for aquitard storage change are likely to be very significant,

inasmuch as the time constants are proportional to storativity and may be of the order of months to years.

3. Method

Measurements with high temporal and spatial resolution of both changes in aquifer hydraulic heads (measured as water level changes in wells) and resulting surface displacements can

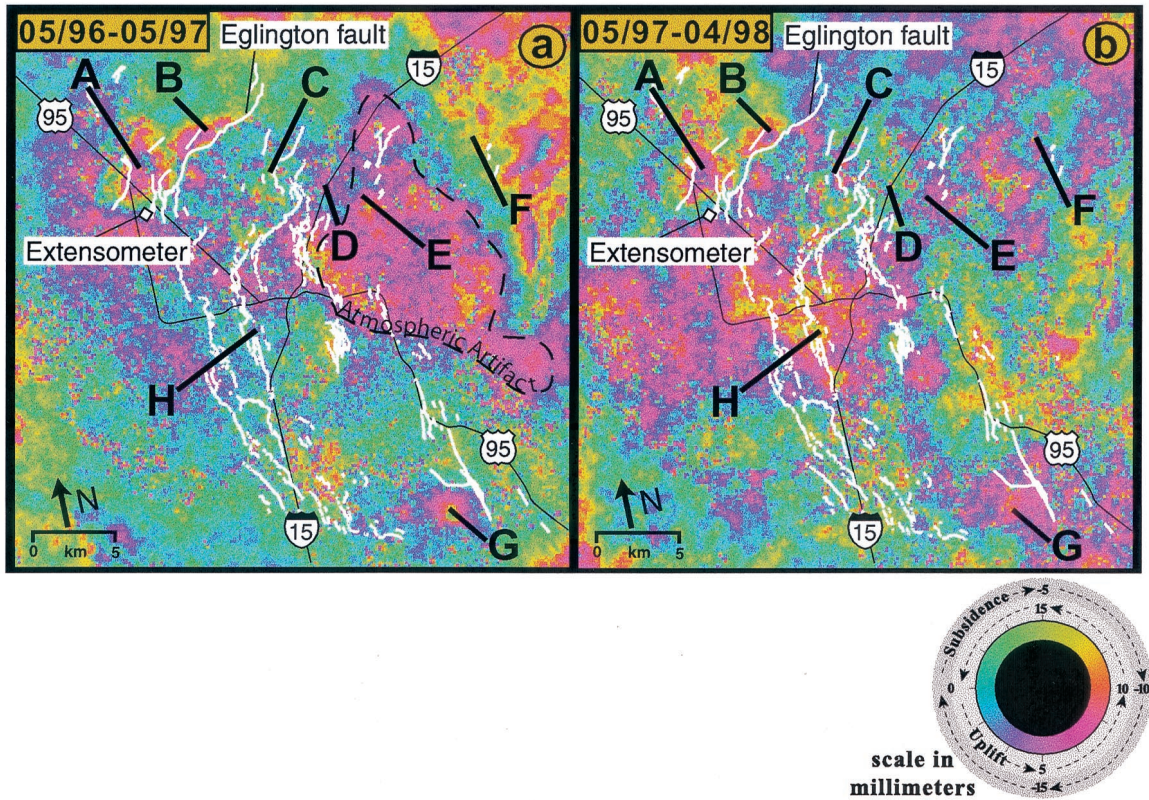


Plate 3. Displacement patterns compared for two consecutive annual periods. Residual subsidence is occurring in (a) the northwest subsidence bowl, while (b) the central subsidence zone shows uplift in 1997–1998. The extended uplift indicated by the outlined area in Plate 3a is probably an atmospheric artifact.

be used to improve estimates of the magnitude and distribution of storage coefficient values. In Las Vegas Valley, coincident measurements of vertical displacement and hydraulic head are available only at the Lorenzi site (Figure 1). Presently, InSAR can map displacements at very high spatial resolution. Using the ERS satellites, this can be done as frequently as every 35 days, the orbit repeat period of the satellites.

InSAR was used initially to measure surface deformation related to a variety of mechanisms such as volcanoes [Massonnet et al., 1995], earthquakes [Massonnet et al., 1993], and glacial flow [Goldstein et al., 1993]. It has also been applied to demonstrate subsidence over active geothermal fields [Massonnet et al., 1997], producing oil fields [Fielding et al., 1998], and aquifer systems [Galloway et al., 1998; Amelung et al., 1999].

Several factors limit the applicability of InSAR. First, differing propagation delays through a troposphere with variable water vapor content can give false deformation signals [Zebker et al., 1997]. Second, temporal decorrelation of the reflective ground surface limits the ability to measure subtle deformation occurring over long time periods: The ground surface in the study area must not undergo too much alteration, on the scale of the radar wavelength (56 mm for ERS) between the two radar acquisitions [Zebker and Villasenor, 1992]. Las Vegas Valley offers favorable conditions for the application of InSAR because of its desert environment. The urban and sparsely vegetated dry surfaces that cover almost the entire Las Vegas Valley preserve the phase coherence of reflected radar signals

over relatively long time periods, even though construction activities may cause a loss of phase coherence locally.

Interferograms are formed from two synthetic aperture radar (SAR) images over an area with nearly identical acquisition geometry. The nearly identical viewing geometry ensures phase coherence between the two radar signals. After carefully coregistering the two images the interferogram is formed by multiplying the first image with the complex conjugate of the second image, yielding the difference phase signal. The resulting map of phase differences can be related to a variety of effects, most importantly displacements within the image, surface topography, and changes in the travel time of the radar signals due to tropospheric delays. The topographic component is removed using a 1-day tandem interferogram [Zebker et al., 1994a].

We used data from both ERS-1 and ERS-2 satellites, processed as 42 interferograms, spanning time periods between 2 and 35 months (Figure 2). The interferograms were used to create the displacement maps shown in Plates 1, 2, and 3, and to construct the time series measurements shown in Figures 3 and 4. We could not use any acquisitions between January 1994 and March 1995, when the ERS-1 satellite was in different orbits. The spatial resolution of the images is initially ~4 m in the along-track direction (azimuth) and 20 m in the across-track direction (range). To eliminate some of the noise and to reduce geometrical distortions we average (multilook) the images, resulting in a 40 m resolution in both azimuth and range.

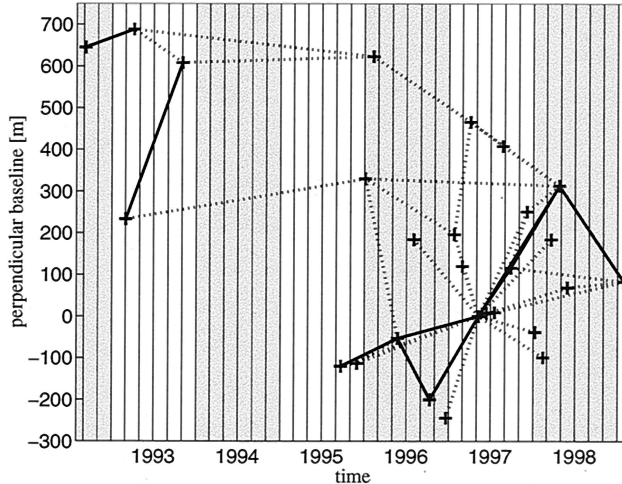


Figure 2. Plot of relative orbit location in space and acquisition times for the radar images used in this study. An interferogram, which is formed by differencing the phase of two image acquisitions, is represented by a line connecting the plus symbols representing those images. The separation of the images in location gives the interferometric perpendicular baseline (B_{\perp}), while the difference in time gives the repeat interval. The solid lines identify the interferograms used for the displacement maps shown in Plates 1, 2, and 3. There are 42 interferograms in this plot. The largest perpendicular baseline is 320 m.

The orbit repeat period of 35 days is the maximum temporal resolution using ERS-2 data.

The accuracy of the range change measurement in radar interferograms decreases with decreasing radar correlation. Correlation in the interferogram depends linearly on the component of the radar baseline perpendicular to the line of sight (called the perpendicular baseline, B_{\perp}) [Zebker *et al.*, 1994b]. Therefore, in the case of exceedingly long B_{\perp} we combined (stacked) two or three interferograms with shorter B_{\perp} to span the same time period in order to maximize the accuracy in the displacement measurements. The longest B_{\perp} used was 320 m (Figure 2). In cases where we compared interferograms with long B_{\perp} to stacks of two or more images covering the same time periods, we found only insignificant differences in displacements and an improvement in the measurement accuracy. Small residual tilts across the image that result from imprecise knowledge of the orbital geometries were corrected by subtracting a least squares plane fit to residual displacement values at a large number of tie points distributed over parts of the valley where no significant subsidence was detected. The measured range changes were projected into the vertical dimension using the incidence angle of the ERS satellites ($\approx 23^{\circ}$).

4. Observations

The available ERS SAR images for Las Vegas Valley cover a wide range of time periods and allow the mapping of the displacement patterns related to groundwater withdrawal with high resolution in both space and time. We concentrated on interferograms covering time periods of up to a few months in order to study the temporal variations in the displacement patterns within individual years. We found that the rates of seasonal displacement exceed the rates of yearly to multiyear displacement almost everywhere. For the following discussion,

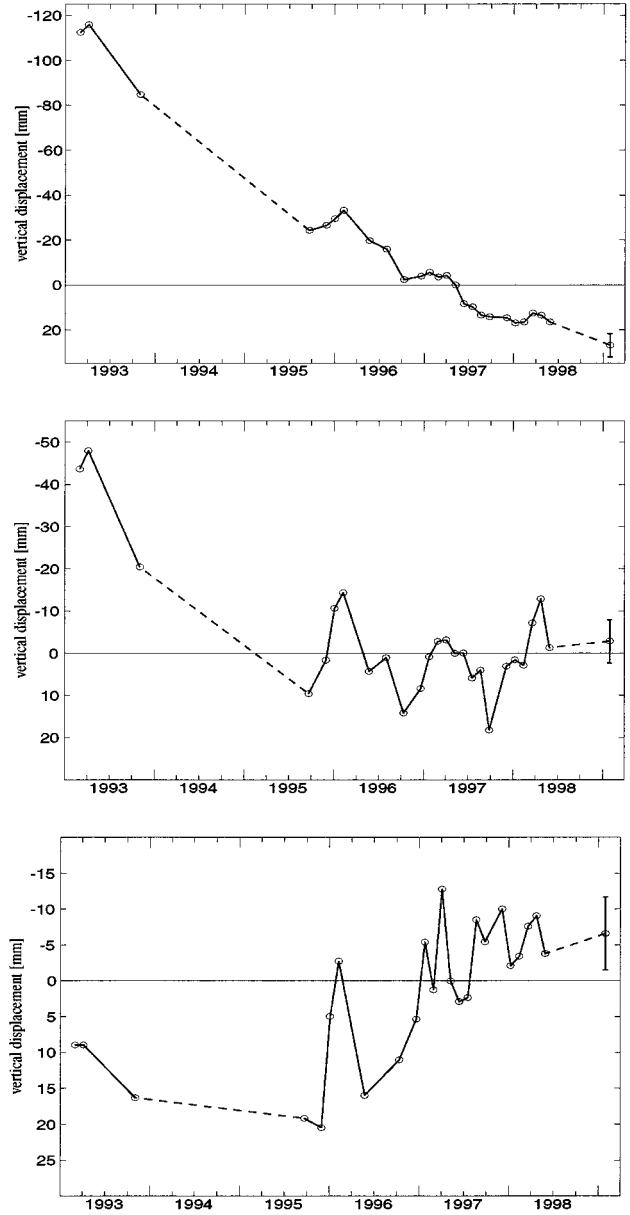


Figure 3. Measured vertical displacements at three locations in Las Vegas Valley: Displacements are shown for (top) the center of the northwest subsidence bowl (area A in Plates 1–3), (middle) the central subsidence zone (2 km east of area H), and (bottom) Whitney Mesa (area G). The displacements are measured in millimeters relative to the May 1997 scene. The estimated accuracy of about ± 5 mm is indicated by the error bar on the most recent data points.

we assume the observed range changes are caused by vertical ground displacements. Observed range increase is referred to as subsidence, and range decrease is referred to as uplift. Following Amelung *et al.* [1999], we refer to the deforming areas in the northwest and central part of Las Vegas Valley as the northwest subsidence bowl and the central subsidence zone, respectively, despite that the observed displacements in the central part of Las Vegas Valley are to a large extent uplift, particularly during the winters. Plates 1, 2, and 3 are displacement maps derived from the acquisition pairs shown as solid lines in Figure 2. Extensive subsidence occurs during the sum-

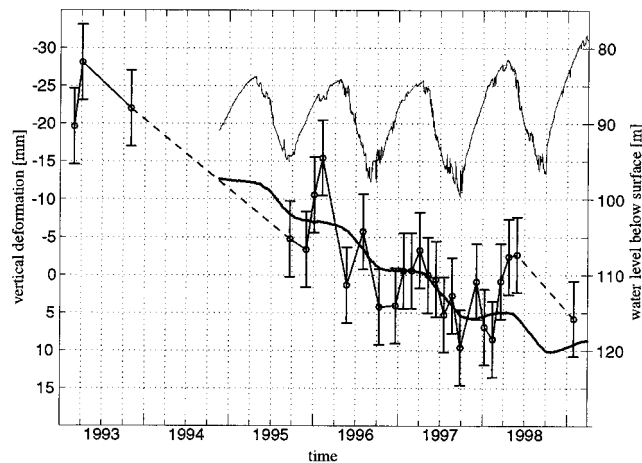


Figure 4. Comparison of vertical displacements measured by InSAR (with error bars) and by the extensometer at the Lorenzi site (bold line) at the southern rim of the subsidence bowl (Figure 1), superposed with aquifer head measured as the depth to water below land surface (thin line) in a well (USGS-PZD) colocated with the extensometer. Although the two measurements are in good agreement, the magnitude of the elastic response is larger for the InSAR measurements. This is likely due to deformation below the depth interval monitored by the extensometer. The error bars for the InSAR measurements are ± 5 mm.

mer over the entire Las Vegas Valley (Plate 1). Though subsidence is greatest in the northwest subsidence bowl, large parts of the central Las Vegas Valley and a few isolated locations in the eastern and southern parts of the valley also subside at detectable rates.

In Las Vegas Valley the summer drawdown season typically occurs during the period April to November, and the remainder of the year constitutes the winter recovery season. Plates 1 and 2 show the measured vertical displacements occurring during four summer seasons (1993, 1996, 1997, and 1998) and four winter seasons (1992–1993, 1995–1996, 1996–1997, and 1997–1998), respectively. The displacement map for the summer of 1998 (Plate 1d) also includes a large part of the following winter season because no SAR acquisition was available in the fall of 1998. In Plates 1–3 one color cycle corresponds to 20

mm of vertical displacement with turquoise being zero displacement (see color scale). Uplift is characterized by blue-red-yellow-green-blue and subsidence is displayed with the reverse color order.

The large-scale subsidence patterns recur in all four summer seasons (Plate 1). However, the northwest subsidence bowl and the central subsidence zone are notably more defined in 1993 (Plate 1a) than in the three more recent summer seasons (Plates 1b–1d). Subsidence during the summer of 1998 is least pronounced (Plate 1d), in particular, in the central subsidence zone. This is, in part, caused by some summer subsidence being offset by some 1998–1999 winter recovery in the interferogram.

During recent winters, subsidence seems to have been largely arrested over the entire valley and extensive uplift can be observed (Plates 2c and 2d), especially in the central subsidence zone. The uplifting areas are larger and the uplift is greater in the most recent winter season 1997–1998 (Plate 1d) than in the earlier 1995–1996 and 1996–1997 images (Plates 2b and 2c). Although the maximum subsidence within the northwest subsidence bowl exceeds 10 mm in all observed winter seasons, the subsidence bowl is less defined in more recent winter seasons (Plates 2b–2d). In the 1997–1998 winter season, there is some localized uplift (blue and pink areas) within the subsidence bowl (Plate 1d).

The maximum subsidence detected within the northwest subsidence bowl (area A) was 42 mm during the summer of 1993, almost twice the maximum subsidence measured in each of the summer seasons in 1996 (24 mm), 1997 (26 mm), and 1998 (24 mm). Peak subsidence of 19 mm, 26 mm, 19 mm, and 12 mm is detected during the winters of 1992–1993, 1995–1996, 1996–1997, and 1997–1998, respectively (Plate 2).

The vertical displacements measured at locations A–H in Plates 1–3 are listed in Table 1. The measured displacements are averages over areas of $\sim 20,000$ m 2 (13 pixels) at each location. The northwest subsidence bowl (areas A and B) shows a dramatic decrease in summer subsidence since 1993 and remains constant from 1996–1998. Winter subsidence in the northwest subsidence bowl has been decreasing linearly since 1992. Areas C through F show localized displacement patterns that may be related to local pumpage or recharge. The magnitudes of seasonal displacement are mostly decreasing with time in these areas. Note that values less than ~ 5 mm

Table 1. Measured Vertical Displacement Magnitudes for the Locations Labeled in Figure 1 and Plates 1–3^a

Area	Summers ^b				Winters ^c				Years ^d	
	Plate 1a	Plate 1b	Plate 1c	Plate 1d	Plate 2a	Plate 2b	Plate 2c	Plate 2d	Plate 3a	Plate 3b
A	+31	+16	+14	+16	+11	+5	+2	-2	+20	+14
B	+24	+11	+10	+17	+9	+5	+2	-1	+14	+9
C	+28	+12	+3	-5	-29	+2	-5	-19	+6	-18
D	+28	-4	+2	-2	-22	+20	+2	-3	-2	+11
E	+1	-12	+14	-1	-30	-12	0	-15	-11	-2
F	+16	+6	-2	+3	-20	-6	+1	-9	+6	-11
G	+7	-6	-6	+3	-9	-3	-11	-3	-16	-9
H	+12	+6	+11	+8	-13	-5	-14	-27	-2	-16

^aAll values are in millimeters. Positive values are subsidence and negative values are uplift. As discussed in section 5, displacement magnitudes smaller than 5 mm are probably insignificant.

^bSummer observation periods are as follows: April 6, 1993 to November 2, 1993 (Plate 1a); May 24, 1996 to October 11, 1996 (Plate 1b); May 9, 1997 to September 26, 1997 (Plate 1c); and April 24, 1998 to January 29, 1999.

^cWinter observation periods are as follows: September 8, 1992 to April 6, 1993 (Plate 2a); September 21, 1995 to May 24, 1996 (Plate 2b); October 11, 1996 to May 9, 1997 (Plate 2c); and September 26, 1997 to April 24, 1998 (Plate 2d).

^dAnnual observation periods are as follows: May 24, 1996 to May 9, 1997 (Plate 3a) and May 9, 1997 to April 24, 1998 (Plate 3b).

probably are not significant, as discussed in the following section. At area E, almost all displacements over the observed periods are uplift. At Whitney Mesa (area G) we observe a curious variation in the displacement trends, from decreasing subsidence (or increasing uplift) from summer 1993 to winter 1996–1997, to comparable displacement magnitudes of opposite trend thereafter. The displacements at area H are typical for the central subsidence zone. Summer subsidence and winter uplift are relatively constant over the entire period of observation (Table 1).

Plate 3 shows measured displacements for two consecutive annual periods. During the first annual period 1996–1997 (Plate 3a), displacements are generally small in the central subsidence zone (including area H), although some small localized areas show subsidence of ~19 mm. The northwest subsidence bowl (including areas A and B) is pronounced with a maximum subsidence of 28 mm. The moderate uplift seen over an extensive area in the eastern part of the valley (labeled) is likely an atmospheric artifact as it is unique to this particular interferogram. During the second annual period 1997–1998 (Plate 3b) a large area of uplift in the central subsidence zone (area H) has a maximum uplift of ~23 mm. The northwest subsidence bowl is somewhat less developed than in the previous year, though the maximum subsidence values are about the same, 29 mm. In some interferograms we observe apparent displacements of the order of 20–30 mm in areas of high relief, especially at Frenchman Mountain, in the east, and the Spring Mountains in the west (Plates 1b, 2d, and 3a). For reasons to be discussed in the next section, these relatively strong signals in the mountainous areas do not discredit the accuracy of the measurements on the valley floor. Figure 3 shows the InSAR-derived displacements at area A in the northwest subsidence bowl, the central subsidence zone (~2 km east of H), and at Whitney Mesa (area G). All measured displacements are shown relative to May 1997. We use this reference image because it is central to the acquired data in time as well as baseline geometry. This allows us to form a large number of displacement maps directly from interferograms involving this scene, rather than stacking interferograms as described in section 3. Where decorrelation due to long temporal baselines or large perpendicular baselines limits our ability to form good interferograms, we combined other interferograms, each with a smaller perpendicular baseline, spanning a shorter time period, to form the displacement map. Each of these displacement maps is represented by one data point in each panel of Figure 3. The error bar shown on the most recent data point in each panel is ± 5 mm to indicate a rough estimate of our achieved accuracy (see section 5). The dashed line segments connect data points that span longer time periods (>5 months) which cannot be used to estimate seasonal fluctuations. In the northwest subsidence bowl (Figure 3, top) we observe a clear subsidence trend on which seasonal fluctuations are superimposed. The subsidence rate is decreasing in recent times. In the central subsidence zone (Figure 3, middle), we observe strong seasonal displacements of the order of 20 mm. Since summer 1995 there has been no significant long-term trend, as the subsidence occurring during the summer seasons is generally recovered as uplift in the following winter season. Thus the earlier subsidence in this area has been essentially arrested for the 4-year period from fall of 1995 to winter of 1998–1999. At Whitney Mesa (Figure 3, bottom) we observe a long-term uplift trend with ~15 mm of uplift from fall of 1995 to winter of 1998–1999. Seasonal fluctuations as

well as the long-term uplift rate are decreasing in more recent times.

5. Accuracy of the Measured Displacements

Very small displacements must be detected reliably if we wish to successfully measure subtle seasonal variations in the displacement patterns in Las Vegas. Although the phase measurements used in the interferometric technique are accurate enough to detect millimeter-level variations, systematic errors introduced by uncertainties in the orbits and changes in tropospheric propagation may bias the InSAR-derived displacements. Because errors due to the imperfect knowledge of the orbits depend on topography and increase with elevation difference, they are less critical in the relatively flat Las Vegas Valley. Small inaccuracies in the satellite orbits introduce roughly linear phase trends across the image [Zebker *et al.*, 1994a]. Thus we are able to correct for these by subtracting a plane from the image that minimizes these tilts in areas where no significant subsidence is observed. As the selection of these areas where subsidence is not expected is somewhat subjective, biases of the resulting displacements may result. However, the residual biases are likely small compared to possible errors introduced by tropospheric delays in the interferograms. We estimate that residual orbit errors are <1 mm over the flat areas of the valley.

Tropospheric errors are a more important concern in seasonal observations by InSAR. Where constant deformation rates persist over considerable time periods, these tropospheric errors can often be decreased by averaging several interferograms. However, in Las Vegas seasonal displacement patterns change too rapidly to use this approach. A signal of localized subsidence and subsequent rebound may not be easily distinguished from tropospheric delay signals. One criterion that is frequently applied in interferometric studies to detect tropospheric artifacts, namely, that they tend to appear only in individual interferograms [Massonnet and Feigl, 1998], could also represent a seasonal subsidence feature unique to one particular season.

Although it is easy to misinterpret some tropospheric signals as deformation (and vice versa), it is, nonetheless, usually possible to differentiate between tropospheric artifacts and subsidence. Most displacement patterns appear at the same area over several seasons, while tropospheric delays, which are statistical in nature, tend not to recur at exactly the same location in consecutive summer or winter seasons. Thus we assume that displacement patterns which are observable over several seasons, such as the subsidence bowl in the northwest or the displacements in the central subsidence zone, are true deformation signals. Conversely, patterns which do not seem to correspond to an area that has been observed before are likely, though not certainly, due to tropospheric delay rather than deformation.

Images with strong tropospheric artifacts are easily identified because of characteristic patterns and scales of tropospheric phenomena. These images can then be excluded from the interpretations or the values drawn from these images can be assigned significantly greater uncertainties. From our experience with the large number of interferograms we processed over the area we estimate that tropospheric delays cause less than ~5 mm error in the measured vertical displacements within the valley, this being the level of easily recognized artifacts.

In some of the interferograms we observe a relatively strong phase signal, corresponding to ~20 to 30 mm, in the areas of high relief surrounding Las Vegas Valley, especially at Frenchman Mountain, in the east, and the Spring Mountains, in the west (Plates 1b, 2d, and 3a). These signals derive from changes in tropospheric conditions as a function of altitude. Electromagnetic waves are affected by temperature as well as moisture content in the troposphere, which are functions of altitude. These tropospheric artifacts can mimic topographic residuals [Delacourt et al., 1998]. On the valley floor this effect does not constitute an important error source, because of the absence of significant topography.

Misinterpretations of measured displacements could also potentially be due to variations in soil moisture content, which can cause measurable displacements of the land surface. Higher soil moisture content may cause relative soil swelling, and lower soil moisture content may cause soil shrinking. Therefore more lawn watering in the summers would lead to swelling, and less watering in the winters would cause shrinkage. However, as we do not observe this effect anywhere outside the subsiding areas, we assume that it is negligible over the entire imaged area.

Because the radar measures changes in range, the distance between the satellite and the ground, to compute equivalent subsidence and uplift, the measured range changes are projected into the vertical dimension under the assumption that no horizontal deformation occurs due to compaction of the aquifer system. According to Helm [1994], inhomogeneities in the aquifer system or steep gradients in the piezometric surface may cause horizontal displacements of the same order of magnitude as the vertical displacements. If there are horizontal displacements with a range component, they will contribute to the error in the measurement. In Las Vegas Valley the occurrence of numerous tensional fissures at land surface provides clear evidence of localized horizontal displacements [Bell and Price, 1991]. It should be noted, though, that because of the relatively steep incidence angle the phase measurement is at least 2.3 times more sensitive to vertical displacements.

6. Comparison of InSAR and Extensometer Measurements

Figure 4 shows the time series of aquifer system compaction measured at the Lorenzi borehole extensometer (Figure 1) located on the southern rim of the northwest subsidence bowl, the InSAR-derived vertical displacements for the same location, and the fluctuation of aquifer head that represents the change in stress driving these displacements. The long-term trends and magnitudes measured by the extensometer and by InSAR are in good agreement. The trends of the seasonal fluctuations also agree very closely. However, the InSAR measurements show seasonal displacements consistently larger than those measured by the extensometer. This difference can be explained by the different thicknesses of deforming sediments that are measured by the two techniques. The extensometer measures vertical compaction and expansion only in the interval from 4 to 244 m below land surface [Pavelko, 2000]. Any compaction or expansion of the aquifer system occurring at depths outside this range is not detected by the extensometer but would be detected by the InSAR measurements.

It is unlikely that the seasonal variations measured by InSAR at the extensometer location are caused by deformation occurring in the uppermost 4 m. The most likely shallow

mechanism would be soil shrinkage and swelling, but two factors argue against this possibility. First, the patterns of seasonal variation are not widespread as one might expect with seasonal climatic variations in soil moisture content. Second, if lawn watering practices were responsible for seasonal changes in soil moisture content we would expect to see relative uplift in summer and relative subsidence in winter, which are not present. Deep wells in the Las Vegas Valley penetrate to depths below 244 m, and more importantly, pressure transients extend into that region, providing the necessary stress changes to cause elastic deformation at these depths.

Another possible source of discrepancy between the two measurements is the measurement "dead band" in the extensometer, the region in which reversing trends in the displacement are not detected. However, the dead band for the Lorenzi extensometer, which ranged between 0.15 and 0.3 mm during the period 1994 to 1999 (M. Pavelko, U.S. Geological Survey, written communication, 1999), is too small to explain the observed differences.

The stepwise seasonal variations in compaction rate measured by the extensometer (Figure 4) reflect elastic seasonal deformation superimposed on nonrecoverable residual compaction attributed to the delayed drainage and fluid-pressure equilibration of thick aquitards. The ongoing residual compaction results in small to no seasonal uplift (rebound) during the periods of groundwater level recovery, followed by accelerated compaction during the periods of drawdown [Riley, 1969; Helm, 1975]. Despite the larger seasonal variations in the InSAR measurements the long-term trend is comparable to the extensometer record. This suggests that thick, slowly draining aquitards within the 244 m depth interval measured by the extensometer are chiefly responsible for the residual compaction occurring at this site. We thus conclude that the larger seasonal variations detected by InSAR are most likely caused by essentially elastic deformation of the aquifer system occurring at depths below 244 m. Altogether, the general agreement between the two methods is very encouraging, while the differences in the seasonal variations are an interesting topic for future investigations.

7. Estimates of Elastic Storage Coefficients

In this section we demonstrate, for six locations in Las Vegas Valley, how estimates of the aquifer system elastic storage coefficients can be derived from the InSAR displacement maps and contemporaneous measurements of water levels in wells, using (2). For this analysis, we assume that the measured range changes are attributed only to vertical displacements of the surface. This assumption may bias the calculated elastic storage coefficients if horizontal displacements are significant. We calculated the elastic storage coefficient at the six observation wells shown in Figure 1. At each site, hydraulic head (measured as the depth to water level in the well below land surface) is monitored in wells penetrating the aquifer system at depths >60 m. Water levels were measured at least every 3 months over the time period spanned by the InSAR observations. The water levels and InSAR-derived ground displacements were used to determine the stress-strain relationship at these sites (Figure 5). Water level variations, plotted on the y axis, represent the applied stresses, and the ground displacements, plotted on the x axis, represent the vertical deformation of the aquifer system. Interferograms with large tropospheric residuals were excluded from the analysis. After Riley [1969] we

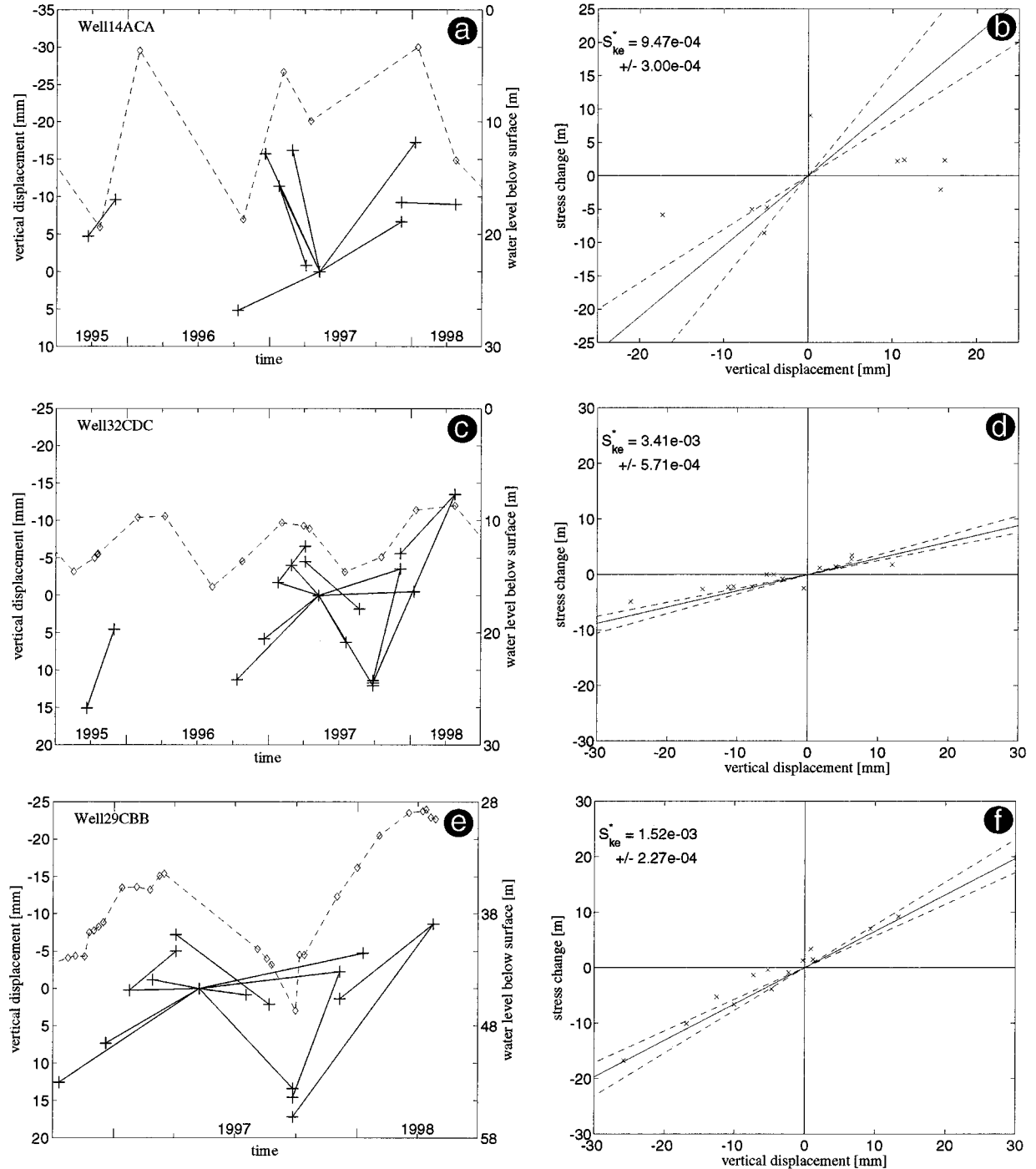


Figure 5. Calculation of the skeletal elastic storage coefficient from stress displacement analysis. On the left are time series plots for water level measurements (diamonds) in meters below land surface and vertical displacements, shown as changes in vertical elevation as measured in the interferograms. Each plus symbol corresponds to a radar acquisition. On the right these data are plotted in a stress-strain diagram. The slope of the solid line is the weighted least squares estimate for the elastic storage coefficient S_{ke}^* . The dashed lines correspond to $\pm\sigma$ values, assuming a 5 mm standard deviation for the displacement measurement and exact interpolated water levels.

computed an estimate of the elastic skeletal storage coefficient from the inverse slope of the best fitting line to the stress displacement data. A weighted least squares approach was used, taking into account that the measurement errors in interferograms that share one radar acquisition are correlated. For each of the wells except the well at the Lorenzi site, where

water level was measured hourly, we linearly interpolated the water level values to the radar acquisition dates. The resulting storage coefficient estimates (Table 2) ranged from 4.2×10^{-4} at well 22BDD in the northwest subsidence bowl to 3.4×10^{-3} at well 32CDC in the central subsidence zone. Table 2 also compares our estimated values with estimates proportional to

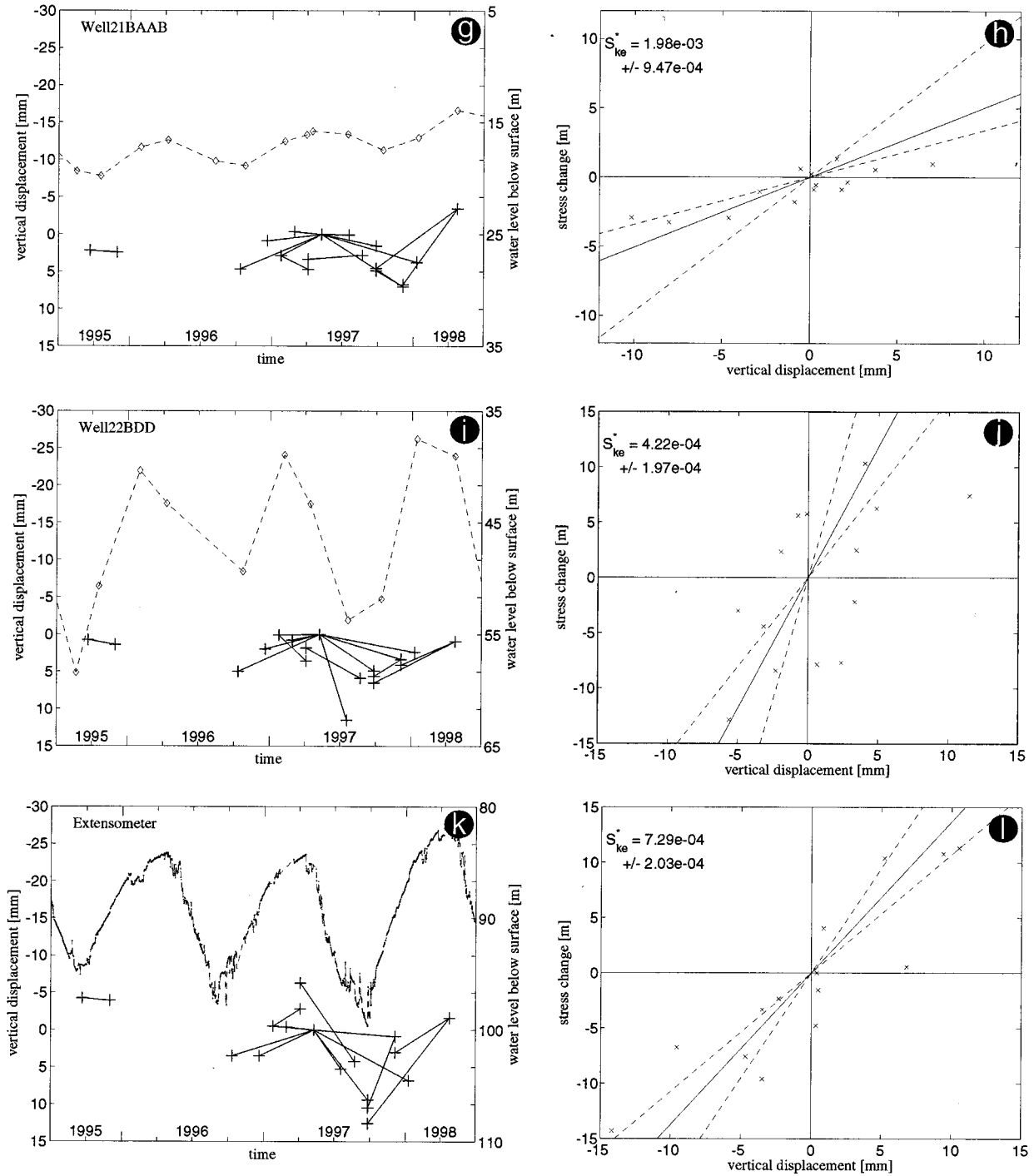


Figure 5. (continued)

an estimate of the saturated thickness of the aquifer system [Todd, 1980]. As an approximation for the saturated thickness we used the thickness of the “Las Vegas Springs aquifer” from Donovan [1996]. This includes most of the “developed-zone aquifers” defined by Morgan and Dettlinger [1996]. This very rough estimate demonstrates very clearly that the typically small variations in saturated thickness limit the estimated storage coefficients to a very narrow range, which cannot explain the observed spatial variability of the displacement field.

We tested the sensitivity of our estimates to the validity of

the assumption that residual, inelastic compaction is negligible by calculating and removing a long-term subsidence trend for each location in the analysis. We found that the resulting estimates were insensitive to the removal of the very small trends and thus conclude that any residual compaction that may still be occurring at these locations does not significantly bias our estimates.

In the described analysis, the water level change measured in the observation wells is assumed to be representative for the aquifer system at the well location. Unfortunately, the vertical

Table 2. Elastic Storage Coefficients, S_{ke}^* , Determined From Displacements Measured by InSAR and Stress Measured as Water Level Change in the Wells Shown in Figure 1^a

Well Name	Monitored Depth Interval, m	S_{ke}^*	S
14ACA	152.4–227.4	9.47×10^{-4}	
32CDC	173.7–198.1	3.41×10^{-3}	4.05×10^{-4}
29CBB	177.1	1.52×10^{-3}	4.80×10^{-4}
21BAAB	61.0–120.4	1.98×10^{-3}	5.40×10^{-4}
22BDD	61.0–121.9	4.22×10^{-4}	5.10×10^{-4}
Extensometer	206.3–209.4	7.29×10^{-4}	4.50×10^{-4}

^aThe aquifer storage coefficients S , derived from the commonly used relation $S = 3 \times 10^{-6}b^*$, where b^* is the saturated thickness of the aquifer system [Todd, 1980], are shown for comparison. (No thickness value was available for well 14ACA). Because the estimates for the saturated thickness of the aquifer system do not vary significantly between the different locations, they limit S to a very narrow range of values. The value for S_{ke}^* determined for the Lorenzi extensometer PZD well from compaction measured by the extensometer is 5.1×10^{-4} (M. Pavelko, written communication, 1999).

distribution of hydraulic head in the aquifer system is generally unknown. If water levels in the observation wells do not represent the local average conditions in the aquifer system, the estimated value for the storage coefficient will be inaccurate. In most cases the values probably are biased toward the low side, because of the delayed propagation of drawdown and recovery from the pumped or recharged aquifers, where water levels are measured. Thus the unknown depth distribution of hydraulic head limits the accuracy of the computed storage coefficients to about one half order of magnitude.

8. Discussion

The displacement maps in Plates 1–3 contain a wealth of information regarding the seasonal deformation of the aquifer system in Las Vegas Valley. Over the last few years, changes in the management of the aquifer system have led to changes in the character of the observed displacements. From late fall to mid-spring, comprehensive groundwater recharge programs are now in effect, primarily in the central and northwestern parts of the valley. These programs, which began in the late 1980s and continue to grow, have helped stabilize groundwater levels in the northwest, which have been recovering slightly since the mid-1990s [Wood, 2000]. Over the longer term, increased water imports since the 1970s from Lake Mead have been used to meet water demand throughout the valley, making it possible to reduce groundwater pumping during the summer months in these areas. As a result, water levels in the central Las Vegas Valley have been recovering since the mid-1990s and are now well above their historic minimum levels [Pavelko et al., 1999]. During the time period 1992–1999 a trend of increasing precipitation has been measured at stations in the recharge source areas of Las Vegas Valley [U.S. Geological Survey, 1992–1999]. This increase in natural recharge could explain some groundwater level recovery and uplift in the valley occurring during this period. However, we believe that this effect is negligible where we observe uplift and water level recovery in the central portion of the valley. In this area, groundwater level recoveries of tens to a hundred feet are occurring in former subsidence areas and near artificial recharge wells. We attribute most of this water level recovery and uplift to artificial recharge.

8.1. Seasonal Deformations

In the northwest subsidence bowl, groundwater levels are recovering and InSAR-derived subsidence rates are declining (Figures 3, 4, and 5i). Using InSAR, Amelung et al. [1999] observed 70–80 mm of subsidence in the northwest bowl between April 1992 and November 1993, a period spanning two summers. We measure a maximum subsidence in the northwest subsidence of 40 mm for the summer of 1993 and a decrease to ~25 mm for each of the summers 1996 through 1998 (Plate 1). There is no significant large-scale deformation detected for the winter of 1996–1997, and some areas within the northwest subsidence bowl show small uplift for the winter of 1997–1998 (Plate 2).

In the central subsidence zone, where Amelung et al. [1999] measured 30–50 mm of subsidence between April 1992 and November 1993, we measure a maximum subsidence of more than 30 mm for the summer of 1993 and somewhat smaller values for the summers, 1996 through 1998 (Plate 1). The surprisingly large uplift of more than 30 mm for the winter of 1997–1998 is larger than for earlier winters, which also clearly show uplift in the central subsidence zone (Plate 2). These results are consistent with elastic expansion of the aquifer system in response to the overall recovery of water levels in the central Las Vegas Valley.

The absence of measurable subsidence in the northwest subsidence bowl during the more recent winter seasons (Plate 2) suggests that residual compaction due to the delayed dissipation of residual excess pore pressure occurring in the thick aquitards is masked by elastic expansion occurring in the thinner and/or more permeable aquitards and in the aquifers due to longer-term seasonal increases in hydraulic head. On the other hand, the net subsidence of about $10\text{--}20 \text{ mm yr}^{-1}$ observed between 1996 and 1998, despite recovering water levels, suggests that some residual compaction is occurring in the aquifer system, causing further permanent subsidence. At the location of the northwest subsidence bowl, Morgan and Dettlinger [1991] estimated an aggregate clay thickness of ~50–100 m within the “developed-zone aquifers” of the valley fill deposits. Little information is available on the thickness of individual aquitards. The boreholes drilled for the piezometers and the extensometer at the Lorenzi site penetrate three thick aquitards, two of which are below the current water table

[Pavelko, 2000]. The presence of these thick aquitards presumably explains the residual compaction measured by the extensometer and perhaps some of the subsidence detected by InSAR in the northwest subsidence bowl.

The same reasoning applied to the absence of significant annual subsidence in the central subsidence zone leads to the conclusion that there is little or no residual compaction and therefore little or no residual excess pore pressure in the aquitards in the central subsidence zone. Water levels in the downtown area of Las Vegas have been stabilized or recovering since the mid-1970s, allowing for dissipation or cancellation of the excess pressure from aquitards. In the central Las Vegas Valley the estimated aggregate clay thickness within the developed-zone aquifers is about 75–150 m [Morgan and Dettinger, 1991], but the thickness of discrete aquitards is unknown to us.

The InSAR-derived displacements suggest that the effective stress changes in the central portion of Las Vegas Valley have been predominantly in the elastic range of aquifer system compressibility since 1995. For aquifer systems, elastic compressibilities are generally 1 or 2 orders of magnitudes smaller than the inelastic compressibilities [Riley, 1998]. Though the magnitude of the maximum observed displacements in the central subsidence zone are seemingly large, they are roughly equivalent to maximum seasonal elastic deformations, 25–30 mm, measured by some extensometers in the Santa Clara [Ireland et al., 1984] and San Joaquin [Poland et al., 1975] Valleys in California. In the northwest subsidence bowl the multiyear compaction rate of more than 10 mm yr⁻¹ is small compared to historical subsidence rates of 63 mm yr⁻¹ measured between 1963 and 1986–1987 [Bell and Price, 1991].

8.2. Land Subsidence From December 1997 to January 1999

The trend of decreasing subsidence rates in the northwest subsidence bowl observed by Amelung et al. [1999] until December 1997 continues through January 1999. The maximum average subsidence rate in the northwest subsidence bowl from December 1997 to January 1999 was 20 mm yr⁻¹, compared to ~25 mm yr⁻¹ in the previous 2 years. This small apparent change in the subsidence rate could be due to measurement error.

The trend of decreasing subsidence rate is also observed in the central subsidence zone, where the average subsidence rate decreased from ~10–15 mm yr⁻¹ from January 1996 to December 1997 to nearly zero from December 1997 to January 1999. Subsidence in the central subsidence zone seems to have been completely arrested during this period.

8.3. Elastic Storage Coefficient Estimates

We computed an estimate of the skeletal elastic storage coefficient of the aquifer system, S_{ke}^* , for six locations in Las Vegas Valley (Table 2). We argue in section 2 that the skeletal elastic storage coefficient is approximately equal to the elastic storage coefficient, S^* , for unconsolidated alluvial deposits in Las Vegas Valley. The computed values are largest for sites in the central part of Las Vegas Valley and smallest for sites in the northwest part of the valley.

Stress-strain analyses using continuously measured displacements and water levels at the Lorenzi extensometer site yield estimates of the elastic storage coefficient of the aquifer system, S_{ke}^* , ranging from 1.1×10^{-4} to 1.3×10^{-3} , averaging 5.1×10^{-4} for a saturated depth interval of 183 m (M. Pavelko, U.S. Geological Survey, written communication, 1999). The

InSAR-derived value, 7.3×10^{-4} , compares favorably within the expected accuracy of the InSAR measurements. The values calculated for the well locations are within the range of elastic storage coefficients estimated for Las Vegas Valley on the basis of a calibrated groundwater flow model [Morgan and Dettinger, 1991] and others determined from pumping tests [Malmberg, 1965]. Given the uncertain vertical distribution of the stress changes in the aquifer system, due largely to the unknown distribution and magnitude of residual excess pore pressures, the elastic storage coefficients calculated on the basis of the InSAR measurements represent first-order estimates with an uncertainty we estimate at about one half order of magnitude. Because of the time lag involved in the equilibration of aquitards a substantial fraction of the aggregate thickness of aquitard material may experience significantly less stress change in a season than is imposed and measured in the interbedded aquifers. Consequently, our seasonally estimated values of S_{ke}^* probably do not fully reflect the material elastic compressibility and thus elastic storage of the aquifer system.

Our calculations were performed for six well locations in Las Vegas Valley. Using additional well data, this analysis could be extended to more locations. If hydraulic heads were calculated from a regional groundwater flow model, the InSAR-derived displacements could be used to create a map of elastic storage coefficients over the aquifer system. These could be used iteratively to improve the groundwater flow model by including the derived storage coefficients. However, these extended analyses are beyond the scope of this paper.

9. Summary and Conclusions

We have shown that InSAR can be used to measure seasonal variations in the displacement field over subsiding or elastically expanding aquifer systems, and how these variations can be used to estimate the elastic storage coefficient over the aquifer system, where measurements of stress change are available. In Las Vegas Valley, the seasonal variations in the displacement patterns are at least of the same order of magnitude as the multiyear displacements. In the central part of the valley, in particular, the observed seasonal fluctuations far exceed the multiyear trend in magnitude. These seasonal displacement signals contain important information about the hydrogeologic properties of the aquifer system and are of considerable value in assessing the effectiveness of groundwater recharge programs. Although the errors in the displacement measurements due to tropospheric delays cannot be effectively corrected for at present, the derived vertical displacements seem to be accurate to ~5 mm. Thus we can use this technique to monitor ongoing subsidence and elastic uplift processes at very high spatial detail over time periods constrained primarily by the orbit repeat cycle of 35 days for the case of ERS-2.

The comparison between the displacements as measured by InSAR at the location of the Lorenzi extensometer located at the southern rim of the northwest subsidence bowl and the extensometer measurements show general agreement in both direction and magnitude of the long-term subsidence. However, the seasonal variations derived from the InSAR measurements are more pronounced than expected from the extensometer data. This difference is best explained by elastic deformation below the base of the extensometer at 244 m. The general agreement between the two techniques supports the use of satellite radar interferometry for the routine monitoring of ongoing subsidence at the basin scale.

During the period 1995–1999, subsidence rates have diminished, stabilized, or reversed in different parts of Las Vegas Valley (Figure 3). The maximum ongoing rate of 25 mm yr⁻¹ occurred in the northwest subsidence bowl. During the winter months this subsidence is almost entirely compensated by elastic expansion of the aquifer system due to recovering hydraulic heads. However, residual compaction in the northwest subsidence bowl will continue despite recovering hydraulic heads until the residual excess pore pressures at the center of the thickest clay beds have completely dissipated. The latter stages of this process may be completely masked by elastic responses in the remainder of the system.

In the central subsidence zone, reduced pumping and artificial recharge seem to have successfully halted further permanent compaction. The deformations in this area are largely elastic, reflecting little or no residual compaction and excess pore pressures, even in the thicker clay beds. The observed seasonal variations of elastic deformation are somewhat larger than expected for Las Vegas Valley. This suggests that the elastic storage values for the aquifer system are somewhat larger than previously thought, as indicated by the values obtained at wells 32CDC, 21BAAB, and 29CBC. With recovering groundwater levels in Las Vegas, future deformations are expected to occur more and more elastically. To the south, in the Whitney Mesa area, almost 30 mm of uplift is indicated, suggesting that deformation in this area has become wholly elastic. Unfortunately, comparable data documenting the presumed recovery of water levels are not presently available.

Las Vegas Valley offers very good conditions for the application of radar interferometry. The absence of dense vegetation and the relatively small amount of precipitation over the valley floor limit the amount of temporal decorrelation and allow formation of interferograms spanning time periods of several years. Similarly favorable conditions prevail over a large number of other aquifer systems in the southwestern United States and in similar climates globally. In these settings the technique used in this paper would be applicable to the study of aquifer system mechanics. The method will become applicable to the study of subsidence in a wider range of environmental settings when radar systems using longer radar wavelengths (L band), which are less prone to decorrelation, become operational in the future.

We have shown that InSAR can be applied to study seasonal variations in the displacement field over aquifer systems at a valley-wide scale with great spatial detail. Where the stress changes in the aquifer system are known from well observations, the InSAR measurements can be used to estimate the elastic storage in the aquifer system, an important parameter for the management of groundwater resources. Although further study of the tropospheric and other systematic biases is necessary to confidently estimate the accuracy of the derived subsidence values, this case study emphasizes the potential for InSAR in hydrogeologic applications.

Appendix A: Aquifer System Storage Coefficients

Deformation of an aquifer system due to changes of the effective stress, $\Delta\sigma_e$ (equation (1)), is governed by the skeletal compressibilities embodied in the aquifer system (aquifers plus aquitards) storage coefficient, S^* :

$$S^* = S_k^* + S_w^*, \quad (A1)$$

$$S_k^* = \rho g b^* \alpha_k, \quad (A2)$$

$$S_k^* = \rho g b^* (\Theta \beta_w), \quad (A3)$$

where S_k^* is the storage due to the compressibility of the aquifer system skeleton, α_k , S_w^* is the storage due to the compressibility of water, β_w , ρ is fluid density, g is gravitational acceleration, b^* is the thickness of the aquifer system, and Θ is the overall porosity of the aquifer system. The star superscript serves to distinguish the lumped aquifer-aquitard properties of the aquifer system. S_k^* can be generally expressed in terms of the skeletal storage coefficient of the aquifers and aquitards that constitute the aquifer system:

$$S_k^* = S_k + S'_k, \quad (A4)$$

where the prime signifies aquitards. If the hydrostratigraphy of the aquifer system is well defined, individual aquifers and aquitards can be included in S_k^* in proportion to their thicknesses and compressibilities. Here we will simply assume two gross fractions, aquifers and aquitards with single-valued properties representative of each fraction.

Because aquitards in an aquifer system can deform elastically and inelastically, two skeletal compressibilities define the aquitard skeletal storage, S'_k , depending on the state of stress:

$$\begin{aligned} S'_k &= \alpha'_{ke} \rho g b', & \sigma_e \leq \sigma_{e(\max)} \\ S'_k &= \alpha'_{kv} \rho g b', & \sigma_e > \sigma_{e(\max)} \end{aligned} \quad (A5)$$

where α'_{ke} and α'_{kv} are the elastic and virgin (inelastic) skeletal compressibilities of the aquitards, respectively, and b' is the thickness of the aquitards. Aquifers deform primarily elastically. Inelastic deformation of the aquifer fraction of the aquifer system is considered to be negligible at the depths of typical groundwater production [Poland, 1984], thus the aquifer skeletal storage is

$$S_k = \alpha_{ke} \rho g b, \quad (A6)$$

where α_{ke} is the elastic skeletal compressibility of the aquifers and b is the thickness of the aquifers. Combining (A2), (A4), (A5), and (A6) for the elastic range of stress, the component of aquifer system storage coefficient (equation (A1)) attributable to elastic deformation of its skeleton can be expressed

$$S_{ke}^* = \rho g (\alpha_{ke} b + \alpha'_{ke} b'), \quad (A7)$$

where S_{ke}^* is the elastic skeletal storage of the aquifer system. Riley [1969] showed that S_{ke}^* could be approximated from measurements of the vertical displacement of the aquifer system and the applied stress by

$$S_{ke}^* = -\frac{\Delta b^*}{\Delta \sigma_e} \rho g \quad (A8)$$

under steady state conditions in the elastic range of deformation. If the total stress remains constant ($\Delta\sigma_T = 0$), we can use (A2) to calculate S_{ke}^* . The total stress can generally be assumed to be constant if the water table in the unconfined aquifer overlying the confined part of the aquifer system does not change significantly. Changes in the water table in the study area during the study period are much smaller than the changes in hydraulic head in the developed confined aquifers, so that this assumption can safely be made.

Acknowledgments. We are grateful to Randell J. Lacznak and Michael T. Pavelko (U.S. Geological Survey, Las Vegas, Nevada) for providing us with water level and extensometer data and valuable

discussions. Scott N. Miller (U.S. Department of Agriculture, Tucson, Arizona), Francis S. Riley (U.S. Geological Survey, Menlo Park, California), Michael T. Pavelko, and an anonymous reviewer provided thoughtful reviews that improved the focus and relevance of this manuscript.

References

- Amelung, F., D. L. Galloway, J. W. Bell, H. A. Zebker, and R. J. Lacznak, Sensing the ups and downs of Las Vegas: InSAR reveals structural control of land subsidence and aquifer-system deformation, *Geology*, 27(6), 483–486, 1999.
- Bell, J. W., and J. G. Price, Subsidence in Las Vegas Valley, 1980–91: Final project report, *U.S. Geol. Surv. Open File Rep. 93-4*, 1991.
- Biot, M. A., General theory of three-dimensional consolidation, *J. Appl. Phys.*, 12, 155–164, 1941.
- Burbey, T. J., Pumpage and water-level change in the principal aquifer of Las Vegas Valley, 1980–90, *Nev. Div. of Water Resour. Inf. Rep. 34*, 224 pp., State of Nev., Carson City, 1995.
- Carrillo-Rivera, J. J., Monitoring of exploited aquifers resulting in subsidence, Example: Mexico City, *Stud. Rep. Hydrol.*, 57, 151–165, 1999.
- Coache, R., Las Vegas Valley water usage report, Clark County, Nevada, 1998, State of Nev. Div. Water Resour. Rep., 137 pp., State of Nev., Carson City, 1999.
- Delacourt, C., P. Briole, and J. Achache, Tropospheric corrections of SAR interferograms with strong topography: Application to Etna, *Geophys. Res. Lett.*, 25, 2849–2852, 1998.
- Donovan, D. J., Hydrostratigraphy and allostratigraphy of the cenozoic alluvium in the northwestern part of Las Vegas Valley, Clark County, Nevada, Master's thesis, Dep. of Geosci., Univ. of Nev., Las Vegas, Aug. 1996.
- Fielding, E. J., R. G. Blom, and R. M. Goldstein, Rapid subsidence over oil fields measured by SAR interferometry, *Geophys. Res. Lett.*, 25(17), 3215–3218, 1998.
- Galloway, D. L., K. W. Hudnut, S. E. Ingebritsen, S. P. Philips, G. Peltzer, F. Rogez, and P. A. Rosen, Detection of aquifer system compaction and land subsidence using interferometric synthetic aperture radar, Antelope Valley, Mojave Desert, California, *Water Resour. Res.*, 34, 2573–2585, 1998.
- Goldstein, R. M., H. Engelhardt, B. Kamb, and R. M. Frolich, Satellite radar interferometry for monitoring ice sheet motion: Application to an Antarctic ice stream, *Science*, 262, 1525–1530, 1993.
- Helm, D. C., One-dimensional simulation of aquifer system compaction near Pixley, California, 1, Constant parameters, *Water Resour. Res.*, 11, 465–478, 1975.
- Helm, D. C., Horizontal aquifer movement in a Theis-Thiem confined system, *Water Resour. Res.*, 30, 953–964, 1994.
- Ireland, R. L., J. F. Poland, and F. S. Riley, Land subsidence in the San Joaquin Valley, California as of 1980, *U.S. Geol. Surv. Prof. Pap. 437-I*, 93 pp., 1984.
- Jacob, C. E., Flow of groundwater, in *Engineering Hydraulics*, edited by H. Rouse, pp. 321–386, John Wiley, New York, 1950.
- Malmberg, G. T., Available water supply of the Las Vegas ground-water basin Nevada, *U.S. Geol. Surv. Water Supply Pap.*, 1780, 116 pp., 1965.
- Massonnet, D., and K. L. Feigl, Radar interferometry and its application to changes in the Earth's surface, *Rev. Geophys.*, 36, 441–500, 1998.
- Massonnet, D., M. Rossi, C. Carmona, F. Adragna, G. Peltzer, K. Feigl, and T. Rabaut, The displacement field of the Landers earthquake, *Nature*, 364, 138–142, 1993.
- Massonnet, D., P. Briole, and A. Arnaud, Deflation of Mount Etna monitored by spaceborne radar interferometry, *Nature*, 375, 567–570, 1995.
- Massonnet, D., T. Holzer, and H. Vadon, Land subsidence caused by the East Mesa geothermal field, California, observed using SAR interferometry, *Geophys. Res. Lett.*, 24, 901–904, 1997.
- Maxey, G. B., and C. H. Jameson, Geology and water resources of Las Vegas, Pahrump, and Indian Springs Valleys, Clark and Nye Counties, Nevada, *Nev. State Eng. Water Resour. Bull.* 5, 121 pp., State of Nev., Carson City, 1948.
- Morgan, D. S., and M. D. Dettinger, Ground-water conditions in Las Vegas Valley, Clark County, Nevada, part 2, Hydrogeology and simulation of ground-water flow, *U.S. Geol. Surv. Water Supply Pap. 2320-B*, 1996.
- Pavelko, M. T., Ground-water and aquifer-system compaction data from the Lorenzi Site, Las Vegas, Nevada, 1994–1999, *U.S. Geol. Surv. Open File Rep.*, 00-362, 26 pp., 2000.
- Pavelko, M., D. Woods, and R. L. Lacznak, Gambling with water in the desert, in *Land Subsidence in the United States*, edited by D. L. Galloway, D. R. Jones, and S. E. Ingebritsen, *U.S. Geol. Surv. Circ.*, 1182, 49–64, 1999.
- Poland, J. F., The coefficient of storage in a region of major subsidence caused by compaction of an aquifer system, *U.S. Geol. Surv. Prof. Pap.*, 424-B, pp. 52–54, 1961.
- Poland, J. F., Guidebook to studies of land subsidence due to ground-water withdrawal, technical report, Unesco, Paris, 1984.
- Poland, J. F., B. E. Lofgren, R. L. Ireland, and R. G. Pugh, Land subsidence in the San Joaquin Valley, California, as of 1972, *U.S. Geol. Surv. Prof. Pap.*, 437-H, 77 pp., 1975.
- Riley, F. S., Analysis of borehole extensometer data from central California, in *Land Subsidence*, vol. 2, edited by L. K. Tison, *Int. Assoc. Sci. Hydrol. Publ.* 89, 423–431, 1969.
- Riley, F. S., Mechanics of aquifer systems—The scientific legacy of Joseph F. Poland, in *Land Subsidence, Case Studies and Current Research*, *Assoc. of Eng. Geol. Spec. Publ.*, vol. 8, edited by J. Borchers, pp. 13–27, Star, Belmont, Calif., 1998.
- Terzaghi, K., *Erdbaumechanik auf Bodenphysikalischer Grundlage*, Deuticke, Vienna, 1925.
- Todd, D. K., *Groundwater Hydrology*, 2nd ed., 535 pp., John Wiley, New York, 1980.
- U.S. Geological Survey, Water resources data, Nevada, water years 1991–1998, *U.S. Geol. Surv. Water Data Rep. NV-91-1 to NV-98-1*, 1992–1999.
- Wood, D. B., Water use and associated effects on ground-water levels, Las Vegas Valley and vicinity, Clark County, Nevada, 1980–95, *Nev. Dep. of Conserv. and Nat. Resour. Water Resour. Inf. Rep. 35*, State of Nev., Carson City, 2000.
- Zebker, H. A., and J. Villasenor, Decorrelation in interferometric radar echoes, *IEEE Trans. Geosci. Remote Sens.*, 30(5), 950–959, 1992.
- Zebker, H. A., C. L. Werner, P. A. Rosen, and S. Hensley, Accuracy of topographic maps derived from ERS-1 interferometric radar, *IEEE Trans. Geosci. Remote Sens.*, 32(4), 823–836, 1994a.
- Zebker, H. A., P. A. Rosen, R. M. Goldstein, G. Andrew, and C. L. Werner, On the derivation of coseismic displacement fields using differential radar interferometry: The Landers earthquake, *J. Geophys. Res.*, 99, 19,617–19,634, 1994b.
- Zebker, H. A., P. A. Rosen, and S. Hensley, Atmospheric effects in interferometric synthetic aperture radar surface deformation and topographic maps, *J. Geophys. Res.*, 102, 7547–7563, 1997.
- F. Amelung, Hawaii Institute of Geophysics and Planetology, University of Hawaii, 2525 Correa Road, Honolulu, HI 96822. (amelung@higp.hawaii.edu)
- D. L. Galloway, U.S. Geological Survey, 6000 J St., Placer Hall, Sacramento, CA 95819-6129. (dlgallow@usgs.gov)
- J. Hoffmann and H. A. Zebker, Department of Geophysics, Stanford University, Mitchell Bldg., Stanford, CA 94305. (joern@pangea.stanford.edu; zebker@stanford.edu)

(Received March 16, 2000; revised December 12, 2000; accepted December 12, 2000.)